23 - Carnoy E., Duvernoy I. and Panosyan G. "Elastoplastic buckling analysis of cylindrical shells under axial compression" in "Recent advances in Nuclear Component testing and theoretical studies on buckling, (ed. G. Baylac), ASME PVP-89, 50-61, 1984

24 - Carnoy E. "Shell finite elements" in "Ispra courses in Structural dynamics", ed Commission of the European Communities, J.R.C. Ispra, Italy, 1983

25 - Handbook of Structural Stability, Ed Column Research Committee of Japan, Corona publishing company LTD., Tokyo, 4-42, 1971

A FINITE ELEMENT FORMULATION FOR THE GEOMETRICALY NON LINEAR ANALYSIS OF SHELLS USING A TOTAL LAGRANGIAN APPROACH.

J. Oliver and E. Oñate

E.T.S. Ingenieros de Caminos, Canales y Puertos
Universidad Politécnica de Cataluña
08034 Barcelona, Spain

SUMMARY

A total Lagrangian formulation for the large displacement-large rotation analysis of shells using finite elements is presented. Different expressions for the strain matrix obtained using various displacement interpolation forms are discussed and details of the obtention of the tangent stiffness matrix are given. Simplifications of the general 3D shell formulation for 2D shells are also presented together with some examples of application.

1. INTRODUCTION

Extensive work has been reported in recent years for the obtention of efficient formulations for the non linear analysis of shells [1]-[14] . Many of the existing formulations allow to follow the deformation of the shell up to large displacement levels but restrict the magnitude of the maximum rotations allowed. However, in many practical engineering problems the large deformation of shells, or shell-like structures, involves very large displacements and rotations and both effects must be properly taken into account in the mathematical formulation. Examples of such situations are very common in mechanical and aeronautical engineering problems. Also, the increasing interest in the application of numerical methods to thin sheet metal forming problems [22] increases the need for reliable formulations which could handle such a potentialy difficult problems in an easy and efficient manner.

The work we present here is an extension of the finite element formulation developed by the authors for the large-displacement-large rotation analysis of 3D and 2D shell structures using a Total Langragian approach. Details of the formulation can be found in references [11], [12], [13] and [14]. The formulation uses "degenerated" shell elements with a local set of Cartesian axes based on the principal directions of the shell for the de-

finition of stresses and strains. Special attention is focussed in this contribution to the analysis of the expressions for the strain-displacement relationship obtained using different finite element interpolations for the basic displacement parameters.

The chapter is divided into the following parts: In the next section details of the geometric and kinematic description for the 3D shell formulation are presented. In section 3 the different interpolation alternatives and the corresponding strain-displacement forms are discussed. Section 4 shows the obtention of the tangent matrix. In section 5 the simplifications of the 3D formulation for axisymmetric shells and arches are presented. Finally, some examples of application are given in section 6.

2. 3-D SHELL FORMULATION : GEOMETRIC AND KINEMATIC DESCRIPTION

2.1. Geometric description.

The middle surface of the shell can be expressed in parametric form as

$$\mathbf{r}_o = [\, x_o(\mu_1, \mu_2),\ y_o(\mu_1, \mu_2),\ z_o(\mu_1, \mu_2)\,]^T \qquad (1)$$

where μ_1 and μ_2 are the principal curvature lines at point 0 of the shell midsurface (see Fig. 1).

Let $\vec{a}$ and $\vec{b}$ be unit vectors tangent to μ_1 and μ_2 in 0, respectively and n the normal vector to the middle surface in 0. Vectors $\vec{a}$, $\vec{b}$ and $\vec{n}$ together with shell parameters r, s and t are defined in Fig. 1.

A second set of orthogonal vectors $\vec{l}$, $\vec{m}$ and $\vec{n}$ is defined at 0 such that $\vec{l}$ is taken as parallel to the global plane xz and also tangent to the shell middle surface, $\vec{n}$ is the normal vector and $\vec{m} = \vec{n} \wedge \vec{l}$ (see Fig. 2).

Vectors $\vec{a}$, $\vec{b}$, $\vec{n}$ define a set of local axes x' , y' , z' associated with the principal curvature lines. On the other hand, vectors $\vec{l}$, $\vec{m}$, $\vec{n}$ define a second set of local axes $\vec{x}$, $\vec{y}$, $\vec{z}$ which is easily identified within the structure.

A point of the shell, P , can be defined by a vector $\vec{r}$ (see Fig. 1) such that we can write in matrix form

$$\mathbf{r}_p = \mathbf{r} = \mathbf{r}_o + t\,\mathbf{n} \qquad (2)$$

where

$$\mathbf{r} = [\, x\ ,\ y\ ,\ z\,]^T \qquad (3)$$

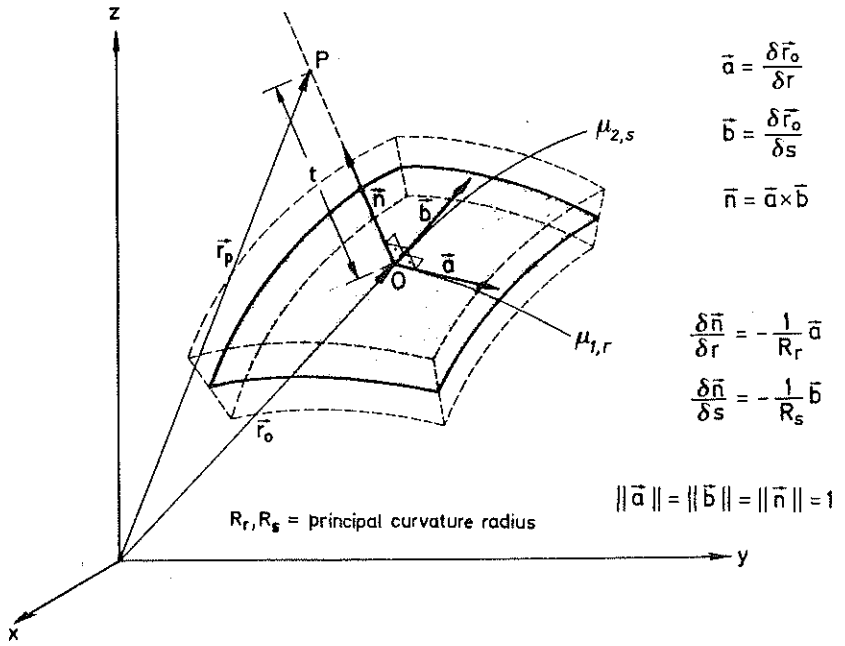

Fig. 1 Definition of shell geometry

Using eq (2) and the relationships shown in Fig. 1 the following expressions can be obtained

$$\left[\frac{\partial (x,y,z)}{\partial (r,s,t)}\right] = \mathbf{T}^T \mathbf{R} \qquad (4)$$

with

$$\mathbf{T} = \left[\, \mathbf{a}\ ,\ \mathbf{b}\ ,\ \mathbf{n}\,\right]^T \quad \text{and} \quad \mathbf{R} = \begin{bmatrix} (1 - \frac{t}{R_r}) & 0 & 0 \\ 0 & (1 - \frac{t}{R_s}) & 0 \\ 0 & 0 & 1 \end{bmatrix} \qquad (5)$$

Additionaly, vectors $\vec{l}$, $\vec{m}$ and $\vec{n}$ can be defined in matrix form as

$$\left[\, \mathbf{l}\ ,\ \mathbf{m}\ ,\ \mathbf{n}\,\right] = \mathbf{T}^T \bar{\mathbf{T}} \quad \text{with} \quad \bar{\mathbf{T}} = \begin{bmatrix} b_y & a_y & 0 \\ -a_y & b_y & 0 \\ 0 & 0 & 1 \end{bmatrix} \qquad (6)$$

in eq (6) $\mathbf{l} = [\, l_x\ ,\ l_y\ ,\ l_z\,]^T$ etc. and the subscripts x, y and z denote components in the global coordinate system.

It is now possible to define the shell geometry in an isoparametric form [16] as:

$$r = \sum_{i}^{n} N_i(\xi, \eta)\, r_{o_i} + \tau \frac{h}{2} n(\xi, \eta) \qquad (7)$$

where r_i is the nodal vector of a finite element mesh discretizing the shell middle surface, n the number of nodes per element, N_i the shape function of node i and ξ and η the normalized isoparametric coordinates. The third normalized coordinate τ is defined as

$$\tau = \frac{2t}{h} \qquad (8)$$

where h is the shell thickness.

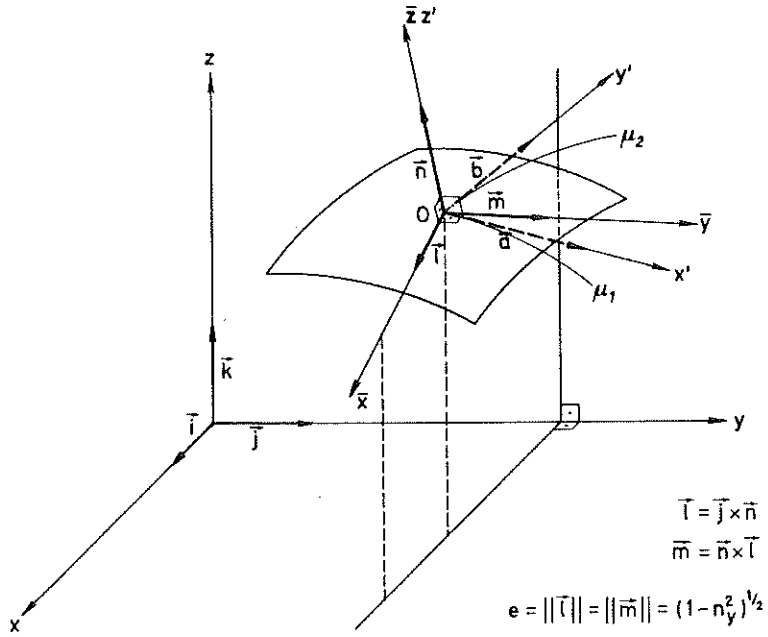

Fig. 2 Different coordinate axes

2.2. Kinematic description.

The displacement vector of a shell point is defined as (see Fig. 3)

$$\vec{u} = \vec{u}_o + t\vec{u}_1 \qquad (9)$$

in (9) $\vec{u}_o$ is the displacement vector of point 0 obtained by projection of P over the shell middle surface $\vec{u}_1$ is the displacement vector of the end of the normal in 0 and t is the distance

between points 0 and P. The vector of "fundamental displacements" is defined in matrix form as

$$p = \begin{Bmatrix} u_o \\ \bar{u}_1 \end{Bmatrix} = \left[u_o , v_o , w_o , \bar{u}_1 , \bar{v}_1 , \bar{w}_1 \right]^T \qquad (10)$$

where u_o , v_o , w_o are the components of u_o in the global coordinate system x , y , z and $\bar{u}_1$, $\bar{v}_1$, $\bar{w}_1$ are the components of $\vec{u}_1$ in the local system $\bar{x}$, $\bar{y}$, $\bar{z}$ (see Fig. 3). The components of p define the displacement of any point of the structure.

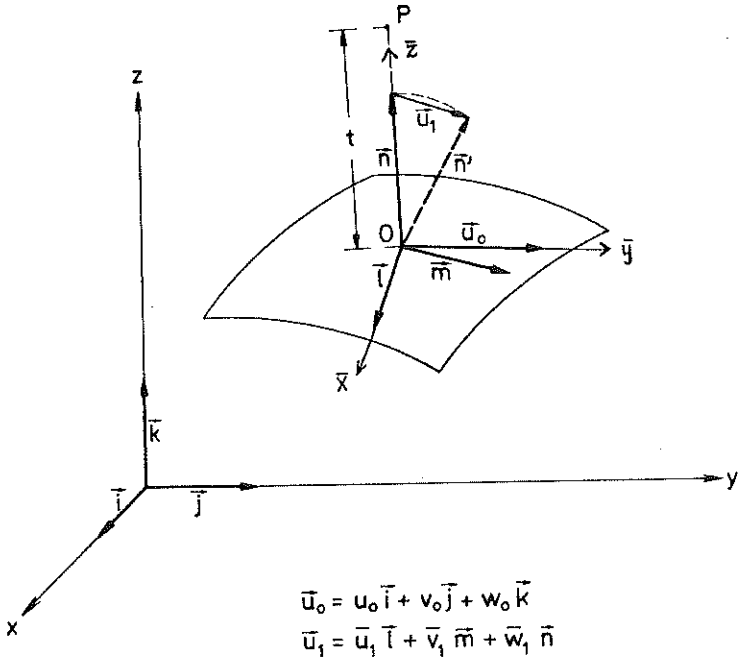

Fig. 3 Displacement vectors

Assuming that the lenght of the normal vector does not change during the deformation we can obtain the nodal components of vector $\vec{u}_1$ as

$$\bar{u}_{1_i} = \left[\frac{-\sin\alpha_i \cos\beta_i}{e_i} , \frac{-\sin\alpha_i \sin\beta_i}{e_i} , \cos\alpha_i - 1 \right]^T \qquad (11)$$

The relationships between angles α_i and β_i and the two no

dal rotations $^{\Theta}\bar{x}_i$ and $^{\Theta}\bar{y}_i$ are shown in Fig. 4b. Note that $^{\Theta}\bar{x}_i$ and $^{\Theta}\bar{y}_i$ are the components of the rotation vector $\vec{\theta}_i$ which expresses the anticlockwise rotation of the normal at node i. Finally, it is worth noting that the definition of nodal rotations is consistent with that of the work done by the bending moments obtained as the scalar product of vector $\vec{M}_i$ and $\vec{\theta}_i$ (see Fig. 4c). Finally, the vector of displacements for node i is defined as

$$a_i = \left[u_{o_i} \; , \; v_{o_i} \; , \; w_{o_i} \; , \; \Theta\bar{x}_i \; , \; \Theta\bar{y}_i \right]^T \qquad (12)$$

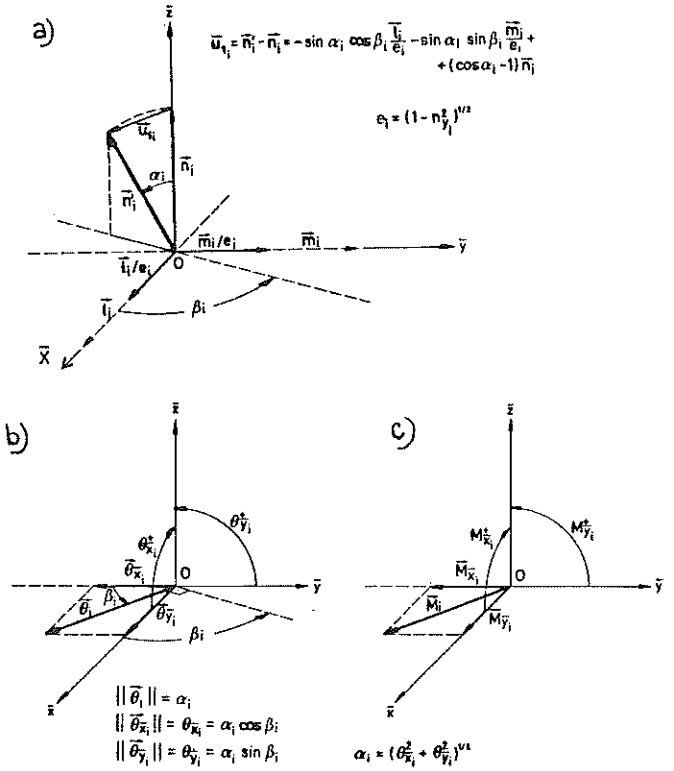

Fig. 4 Definition of nodal rotations

3. STRAIN-DISPLACEMENT RELATIONSHIP. DIFFERENT INTERPOLATION ALTERNATIVES.

The vector of displacement gradients at a point can be defined as

$$g = \begin{Bmatrix} g_1 \\ g_2 \\ g_3 \end{Bmatrix} = \begin{Bmatrix} \frac{\partial}{\partial x'} & u' \\ \frac{\partial}{\partial y'} & u' \\ \frac{\partial}{\partial z'} & u' \end{Bmatrix} \qquad (13)$$

with (14)

$$g_1 = \left[g_1 \; , \; g_2 \; , \; g_3 \right]^T \; , \; g_2 = \left[g_4 \; , \; g_5 \; , \; g_6 \right]^T \text{ and } g_3 = \left[g_7 \; , \; g_8 \; , \; g_9 \right]^T$$

In (13) $u' = [u' \; , \; v' \; , \; w']^T$ is the displacement vector of the point referred to the local axes x' , y' , z' of Fig.2.

The Green strain vector can be written (neglecting the contribution of the thickness strain in the deformation) as

$$\epsilon = \begin{Bmatrix} \epsilon_{x'} \\ \epsilon_{y'} \\ \gamma_{x'y'} \\ \gamma_{x'z'} \\ \gamma_{y'z'} \end{Bmatrix} = \begin{Bmatrix} g_1 + \tfrac{1}{2}(g_1^2 + g_2^2 + g_3^2) \\ g_5 + \tfrac{1}{2}(g_4^2 + g_5^2 + g_6^2) \\ g_2 + g_4 + g_1 g_4 + g_2 g_5 + g_3 g_6 \\ g_3 + g_7 + g_1 g_7 + g_2 g_8 + g_3 g_9 \\ g_6 + g_8 + g_4 g_7 + g_5 g_8 + g_6 g_9 \end{Bmatrix} \qquad (15)$$

vector **g** can be obtained in terms of the fundamental displacement vector as [12]

$$g = \begin{bmatrix} C_r T \frac{\partial}{\partial r} & \vdots & tC_r \left(\Delta_1 + \bar{T} \frac{\partial}{\partial r} \right) \\ C_s T \frac{\partial}{\partial s} & \vdots & tC_s \left(\Delta_2 + \bar{T} \frac{\partial}{\partial s} \right) \\ 0 & \vdots & \bar{T} \end{bmatrix} p = [L_1 \; , \; L_2] \, p = L p \qquad (16)$$

with $C_r = \dfrac{1}{1 - \frac{t}{R_r}}$ $\qquad$ $C_s = \dfrac{1}{1 - \frac{t}{R_s}}$

$$\Delta_1 = \frac{1}{R_r} \begin{bmatrix} 0 & n_y & -1 \\ -n_y & 0 & 0 \\ b_y & a_y & 0 \end{bmatrix} \; , \; \Delta_2 = \frac{1}{R_s} \begin{bmatrix} n_y & 0 & 0 \\ 0 & n_y & -1 \\ -a_y & b_y & 0 \end{bmatrix} \qquad (17)$$

The relationship between the strain vector and the vector of nodal displacements depends on the finite element interpolation used for the displacement field. Here different alternatives are possible and some of these are discussed in next sections.

3.1. Option 1 : Interpolation of the vector of fundamental displacements.

The six components of vector $\mathbf{p}$ of eq (10) can be interpolated i.e.

$$\mathbf{p} = \sum^{n} N_i \, \mathbf{p}_i \tag{18}$$

where $\mathbf{p}_i^T = \left[\mathbf{u}_{o_i}^T , \; \vec{\mathbf{u}}_{1_i}^T \right]$ are the nodal values of $\mathbf{p}$, $N_i = N_i \mathbf{I}_6$ and $\mathbf{I}_6$ is the 6 x 6 unit matrix.

Substituting eq (18) in (16) we have

$$\mathbf{g} = \mathbf{L} \sum^{n} N_i \, \mathbf{p}_i = \sum^{n} \mathbf{M}_i \, \mathbf{p}_i \tag{19}$$

where

$$\mathbf{M}_i = \mathbf{L} \, N_i = \left[L_1 N_i , \; L_2 N_i \right] = \left[\vec{\mathbf{M}}_i , \; \vec{\vec{\mathbf{M}}}_i \right] \tag{20}$$

The incremental form of eq (18) and (19) can be written as

$$\delta \mathbf{p}_i = \begin{bmatrix} \mathbf{I}_3 & \mathbf{0} \\ \mathbf{0} & \mathbf{V}_i \end{bmatrix} \delta \mathbf{a}_i = \mathbf{C}_i \, \delta \mathbf{a}_i \tag{21}$$

$$\delta \mathbf{g} = \sum^{n} \mathbf{M}_i \, \delta \mathbf{p}_i = \sum^{n} \mathbf{M}_i \, \mathbf{C}_i \delta \mathbf{a}_i = \sum^{n} \mathbf{G}_i \delta \mathbf{a}_i \tag{22}$$

where $\mathbf{G}_i = \mathbf{M}_i \, \mathbf{C}_i$ (23)

Finally, the incremental relationship between Green strains and nodal displacements is obtained from eqs (15) and (22) as

$$\delta \boldsymbol{\varepsilon} = \mathbf{A} \, \delta \mathbf{g} = \mathbf{A} \sum^{n} \mathbf{G}_i \, \delta \mathbf{a}_i = \sum^{n} \mathbf{B}_i \, \delta \mathbf{a}_i \tag{24}$$

where the strain matrix $\mathbf{B}_i = \mathbf{A} \, \mathbf{G}_i$. Explicit forms of matrices $\mathbf{M}_i$, $\mathbf{C}_i$, $\mathbf{G}_i$, $\mathbf{A}$ and $\mathbf{B}_i$ can be found in references [11] and [12].

3.2. Option 2: Interpolation of global components of vector $\mathbf{p}$.

The vector of fundamental displacements is redefined as

$$\hat{\mathbf{p}} = \left[\mathbf{u}_o^T , \; \mathbf{u}_4^T \right]^T \tag{25}$$

where $\mathbf{u}_4$ refer to the components of vector $\vec{\mathbf{u}}_1$ in the global coordinate system. The new vector of fundamental displacements is interpolated as

$$\hat{\mathbf{p}} = \sum^{n} N_i \, \hat{\mathbf{p}}_i \tag{26}$$

It can be shown that the relationship between vector $\mathbf{p}$ and

$\hat{\mathbf{p}}$ is given by

$$\mathbf{p} = \hat{\mathbf{T}} \, \hat{\mathbf{p}} \tag{27}$$

where

$$\hat{\mathbf{T}} = \begin{bmatrix} \mathbf{I}_3 & \mathbf{0} \\ \mathbf{0} & \begin{bmatrix} \mathbf{l}^T \\ \mathbf{m}^T \\ \mathbf{n}^T \end{bmatrix} \end{bmatrix} \tag{28}$$

From eqs (16), (27) and (26) it can be obtained

$$\delta \mathbf{g} = \mathbf{L} \, \delta \mathbf{p} = \mathbf{L} \, \hat{\mathbf{T}} \, \delta \hat{\mathbf{p}} = \mathbf{L} \sum^{n} \hat{\mathbf{T}} \, N_i \delta \hat{\mathbf{p}}_i = \sum^{n} \hat{\mathbf{M}}_i \, \delta \hat{\mathbf{p}}_i \tag{29}$$

where

$$\hat{\mathbf{M}}_i = \mathbf{L} \, (\hat{\mathbf{T}} \, N_i) \tag{30}$$

The incremental relationship between $\hat{\mathbf{p}}_i$ and the displacement vector $\mathbf{a}_i$ can be obtained as

$$\delta \hat{\mathbf{p}}_i = \hat{\mathbf{T}}_i^T \, \delta \mathbf{p}_i = \hat{\mathbf{T}}_i^T \, \mathbf{C}_i \, \delta \mathbf{a}_i = \hat{\mathbf{C}}_i \, \delta \mathbf{a}_i \tag{31}$$

where

$$\hat{\mathbf{C}}_i = \hat{\mathbf{T}}_i^T \mathbf{C}_i \tag{32}$$

Substitution of eq (31) in (29) yields

$$\delta \mathbf{g} = \sum^{n} \hat{\mathbf{M}}_i \hat{\mathbf{C}}_i \, \delta \mathbf{a}_i = \sum^{n} \hat{\mathbf{G}}_i \, \delta \mathbf{a}_i \tag{33a}$$

with

$$\hat{\mathbf{G}}_i = \hat{\mathbf{M}}_i \hat{\mathbf{C}}_i \tag{33b}$$

Finally, matrix $\mathbf{B}_i$ is obtained by

$$\mathbf{B}_i = \mathbf{A} \, \hat{\mathbf{G}}_i \tag{33c}$$

3.3. Option 3: Interpolation of the displacement vector.

Vector $\mathbf{a}$ of eq (12) can be interpolated as

$$\mathbf{a} = \sum^{n} \bar{\mathbf{N}}_i \mathbf{a}_i \tag{34}$$

with $\bar{\mathbf{N}}_i = N_i\, \mathbf{I}_5$ being $\mathbf{I}_5$ the 5 x 5 unit matrix. Using eqs (21) and (34) we can write

$$\delta \mathbf{p} = \mathbf{C}\, \delta \mathbf{a} = \mathbf{C} \sum^{n} \bar{\mathbf{N}}_i\, \delta \mathbf{a}_i = \sum^{n} \bar{\mathbf{C}}_i \delta \mathbf{a}_i \tag{35}$$

where

$$\bar{\mathbf{C}}_i = \mathbf{C}\, \bar{\mathbf{N}}_i \quad \text{and} \quad \mathbf{C} = \begin{bmatrix} \mathbf{I}_3 & \mathbf{0} \\ \mathbf{0} & \mathbf{V} \end{bmatrix} \tag{36}$$

Matrix $\mathbf{C}$ of eq (36) is a generalization of $\mathbf{C}_i$ of eq (21) for any point of the structure. The explicit expression of $\mathbf{V}$ in (36) can be directly obtained from that of $\mathbf{V}_i$ given in reference [12] simply substituting the nodal angles α_i, β_i by α, β respectively.

From eqs (16) and (35) it can be easily found

$$\delta \mathbf{g} = \mathbf{L}\, \delta \mathbf{p} = \sum^{n} \mathbf{L}\, \bar{\mathbf{C}}_i\, \delta \mathbf{a}_i = \sum^{n} \bar{\mathbf{G}}_i\, \delta \mathbf{a}_i \tag{37}$$

where

$$\bar{\mathbf{G}}_i = \mathbf{L}\, \bar{\mathbf{C}}_i \tag{38}$$

Finally, matrix $\mathbf{B}_i$ can be obtained following identical steps shown in eq (24) using matrix $\bar{\mathbf{G}}_i$ instead of $\mathbf{G}_i$.

3.4. Option 4: Interpolation of the three global displacements and the two angles α and β.

We will finally considered here the option in which vector $\mathbf{u}_o$ and the two angles α and β of Fig. 4 are interpolated. Thus we define vector $\mathbf{b}$ as

$$\mathbf{b} = [\mathbf{u}_o^T\ ,\ \alpha\ ,\ \beta\ ]^T = \sum^{n} \bar{\mathbf{N}}_i \mathbf{b}_i \tag{39}$$

where $\mathbf{b}_i = [\mathbf{u}_{o_i}^T, \alpha_i, \beta_i]^T$ and $\mathbf{N}_i = N_i \mathbf{I}_5$

From the relationships in Fig. 4 and eq (39) we can obtain

$$\delta \mathbf{p} = \mathbf{S}\, \delta \mathbf{b} = \mathbf{S} \sum^{n} \bar{\mathbf{N}}_i \delta \mathbf{b}_i = \mathbf{S} \sum^{n} \bar{\mathbf{N}}_i \mathbf{R}_i\, \delta \mathbf{a}_i = \sum^{n} \mathbf{C}_i^{*} \delta\, \mathbf{a}_i \tag{40}$$

where

$$\mathbf{C}_i^{*} = \mathbf{S}\, \bar{\mathbf{N}}_i \mathbf{R}_i \tag{41}$$

with

$$\mathbf{S} = \begin{bmatrix} \mathbf{I}_3 & \mathbf{0} \\ \mathbf{0} & \mathbf{F} \end{bmatrix} \quad \text{and} \quad \mathbf{R}_i = \begin{bmatrix} \mathbf{I}_3 & \mathbf{0} \\ \mathbf{0} & \mathbf{H}_i \end{bmatrix} \tag{42}$$

Matrices $\mathbf{F}$ and $\mathbf{H}_i$ in (42) are given by

$$\mathbf{F} = \begin{bmatrix} -\frac{1}{e}\cos\alpha\cos\beta & \frac{1}{e}\sin\alpha\ \mathrm{sen}\beta \\ -\frac{1}{e}\cos\alpha\sin\beta - \frac{i}{e}\sin\alpha\cos\beta & \\ -\sin\alpha & 0 \end{bmatrix};\quad \mathbf{H}_i = \begin{bmatrix} \cos\beta_i & \sin\beta_i \\ \frac{-\sin\beta_i}{\alpha_i} & \frac{\cos\beta_i}{\alpha_i} \end{bmatrix} \tag{43}$$

Finally, from eqs (16) and (40) we obtain

$$\delta \mathbf{g} = \mathbf{L}\, \delta \mathbf{p} = \mathbf{L} \sum^{n} \mathbf{C}_i^{*} \delta\, \mathbf{a}_i = \sum^{n} \mathbf{G}_i^{*} \delta\, \mathbf{a}_i \tag{44}$$

and matrix $\mathbf{B}_i$ is obtained using $\mathbf{G}_i^{*}$ instead of $\mathbf{G}_i$ in eq (24).

3.5. Comparison of the different interpolation options.

It can be deduced from previous sections that for practical purposes the main difference between the four finite element interpolations alternatives lays in the expression giving the matrix relating the incremental form of the displacement gradient and the nodal displacement vectors. A summary of the different expressions for such a matrix obtained in previous sections are given below

Option 1

$$\mathbf{G}_i = (\mathbf{L}\, \mathbf{N}_i)\mathbf{C}_i \tag{45}$$

Option 2

$$\hat{\mathbf{G}}_i = \mathbf{L}\, (\hat{\mathbf{T}}\, \mathbf{N}_i)\, \hat{\mathbf{T}}_i^T \mathbf{C}_i \tag{46}$$

Option 3

$$\bar{\mathbf{G}}_i = \mathbf{L}\, (\mathbf{C}\, \bar{\mathbf{N}}_i) \tag{47}$$

Option 4

$$\mathbf{G}_i^{*} = \mathbf{L}\, (\, \mathbf{S}\, \bar{\mathbf{N}}_i\, \mathbf{R}_i) \tag{48}$$

It can be clearly deduced from above expressions that option 1 yields the simpler procedure for the obtention of matrix $\mathbf{G}$, since the gradient operator $\mathbf{L}$ is applied only to the shape function matrix $\mathbf{N}_i$. All the other options imply the application of $\mathbf{L}$ to a non constant transformation matrix and additional matrix multiplications which, in conclusion, make the computation of $\mathbf{G}$ more costly and complicated. Option 1, therefore, comes

out as the most efficient procedure and it has been used for the examples presented in section 6.

4. COMPUTATION OF THE TANGENT MATRIX.

The discretized equilibrium equations for the structure can be obtained via the virtual work expression [16]. Following standard procedures we can write in matrix form

$$\Psi(a) = p(a) - r(a) = 0 \tag{49}$$

where $\Psi(a)$ is the residual force vector and $p(a)$ and $r(a)$ are the internal force and equivalent external nodal force vectors, respectively. For total Lagrangian problems we can write eq (49) for the ith node as

$$\psi_i(a) = \int_V B_i^T \sigma dv - r_i(a) = 0 \tag{50}$$

where B_i is the strain matrix given in eq (24), σ is the second Piola-Kirchhoff stress vector and V is the underformed volume of the structure. In this work we have assumed conservative loading, i.e. $r_i(a) = r_i$. The expressions of r_i for various types of loading can be found in [12].

Eq (49) is a non linear system of equations which can be solved using any of the existing iterative algorithms [15], [16]. We have chosen here a standard Newton-Raphson procedure [16] for which the displacement increment vector for the nth iteration is given by

$$\Delta a^n = -\frac{\partial \psi(a^n)}{\partial a}\,\psi(a^n) = -K_T(a^n)\,\psi(a^n) \tag{51}$$

The updated displacement field is then calculated as $a^{n+1} = a^n + \Delta a^n$. Iterations stop when eq (49) is satisfy (in an error norm sense).

For conservative loading a typical submatrix of K_T linking nodes i and j can be obtained by

$$K_{T_{ij}} = \frac{\partial p_i}{\partial a_j} \tag{52}$$

It can be shown that $K_{T_{ij}}$ can be given by [12]

$$K_{T_{ij}} = K_{ij}^L + K_{ij}^{\sigma_I} + K_{ij}^{\sigma_{II}} \tag{53}$$

where

$$K_{ij}^L = \int_V B_i^T D B_j \, dv \tag{54}$$

$$K_{ij}^{\sigma_I} = \int_V G_i^T S G_j \, dv \tag{55}$$

$$K_{ij}^{\sigma_{II}} = 0 \quad \text{for} \quad i \neq j \quad \text{and} \quad K_{ii}^{\sigma_{II}} = \begin{bmatrix} 0 & 0 \\ 0 & H_i \end{bmatrix} \tag{56}$$

In eq (54) D is the constitutive matrix relating the second Piola-Kirchhoff stress vector and the Green strain vector. On the other hand, matrix S of eqs (55) is given by

$$S = \begin{bmatrix} \sigma_{x'} I_3 & \tau_{x'y'} I_3 & \tau_{x'z'} I_3 \\ & \sigma_{y'} I_3 & \tau_{y'z'} I_3 \\ \text{symm.} & & 0 \end{bmatrix} \tag{57}$$

Finally, matrix H_i of eq (56) is obtained for option 1 of section 3.1 as

$$H_i = \int_V \left[\frac{\partial V_i^T}{\partial \theta_{\bar{x}_i}} F_i \;,\; \frac{\partial V_i^T}{\partial \theta_{\bar{y}_i}} F_i \right] dv \tag{58}$$

with

$$F_i = \bar{\bar{M}}_i A^T \sigma \tag{59}$$

Explicit expressions of matrices $\frac{\partial V_i}{\partial \theta_{\bar{x}_i}}$ and $\frac{\partial V_i}{\partial \theta_{\bar{y}_i}}$ can be found in [11] and [12].

All the integrals of the different tangent stiffness matrices have been evaluated using a Gauss-Legendre numerical integration quadrature. Details of the numerical integration transformations and of the computation of the curvature radii and derivatives of shape functions which appear in different matrices can be found in [11], [12].

5. SIMPLIFICATIONS FOR AXISYMMETRIC SHELLS AND ARCHES.

The general non linear shell formulation presented in previous sections can be easily simplified for the analysis of axisymmetric shells or arch/frame type structures. Only details of the main simplifications will be given here. More extensive details can be found in [13].

5.1. Geometric description.

A global coordinate system is chosen such that the plane which contains the middle line of the structure coincides with the global plane xz. For axisymmetric shells the middle line of a meriditional section is considered (see Fig. 5)

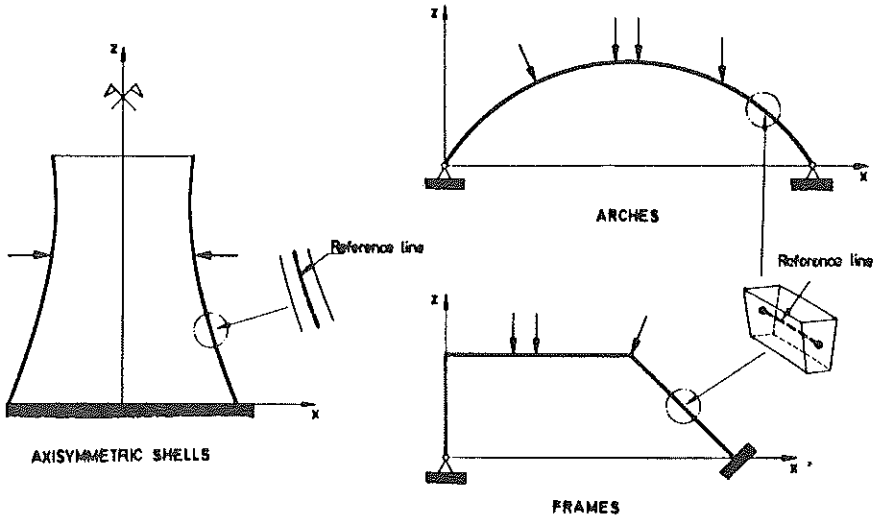

Fig. 5 Axisymmetric shells, arches and frames

Vectors a and n of Fig. 1 are now defined by

$$\mathbf{a} = [\cos\phi\ ,\ \sin\phi\ ]^T \quad , \quad \mathbf{b} = [-\sin\phi\ ,\ \cos\phi\ ]^T \qquad (60)$$

It can be seen that coordinates y and s of the general shell formulation need not to be considered. Also local axes x' y' z' and $\bar{x}\ \bar{y}\ \bar{z}$ of Fig. 2 coincide all now with the set of axes defined by vectors **a** , **b** (not used) and **n** (see Fig. 6). Thus, direct use can be made of all geometrical relations given in section 2.1 simply noting that coordinates y and s are not needed and the coincidence of coordinate systems referred. In consequence, matrices **T** , **R** and $\bar{\mathbf{T}}$ of eqs (5) and (6) are now obtained as

$$\mathbf{T} = \begin{bmatrix} \cos\phi & \sin\phi \\ -\sin\phi & \cos\phi \end{bmatrix} \quad , \quad \mathbf{R} = \begin{bmatrix} (1-\frac{t}{R}) & o \\ o & 1 \end{bmatrix} , \quad \bar{\mathbf{T}} = \mathbf{I}_2 \qquad (61)$$

where $\mathbf{I}_2$ is the 2 x 2 unit matrix.

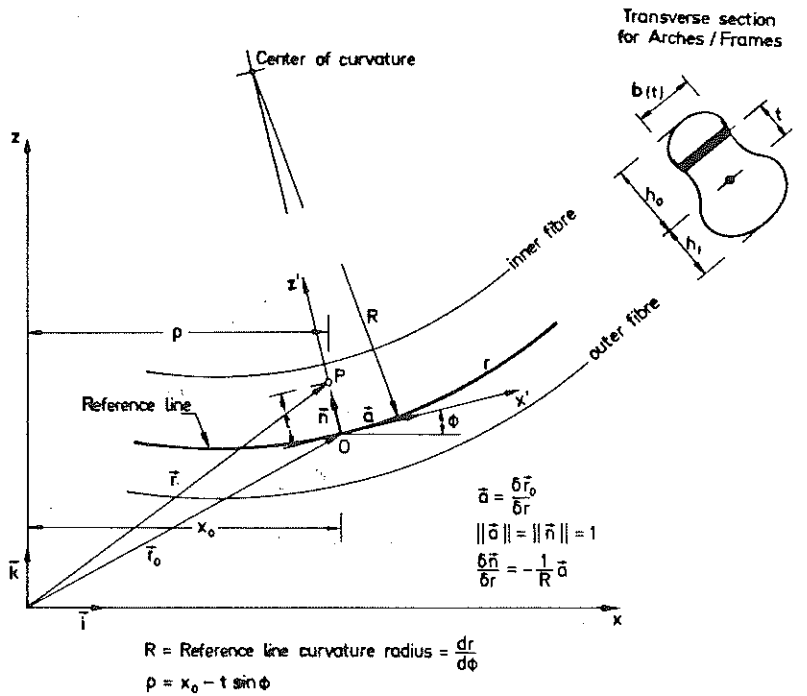

Fig. 6 Geometric description of reference line

On the other hand, eq (7) is again valid with $N_i = N_i(\xi)$ and the value of the normalised coordinate τ given by

Axisymmetric shells	Arches
$\tau = \frac{2t}{h}$	$\tau = \frac{h_1 - h_o + 2t}{h}$ (62)

where distances h_1 and h_o can be seen in Fig. 6 .

6.2. Kinematic description.

Eqs (9) and (10) are again applicable (see Fig. 7) with

$$\mathbf{u}_o = [\, u_o\ ,\ w_o\ ]^T \qquad (63)$$

and

$$\bar{\mathbf{u}}_{1_i} = [-\sin\theta_i\ ,\ (\cos\theta_i - 1)\,]^T \qquad (64)$$

The vector of displacements of node i is defined now as

$$a_i^T = [\, u_{o_i}^T \;,\; \theta_i \,] \tag{65}$$

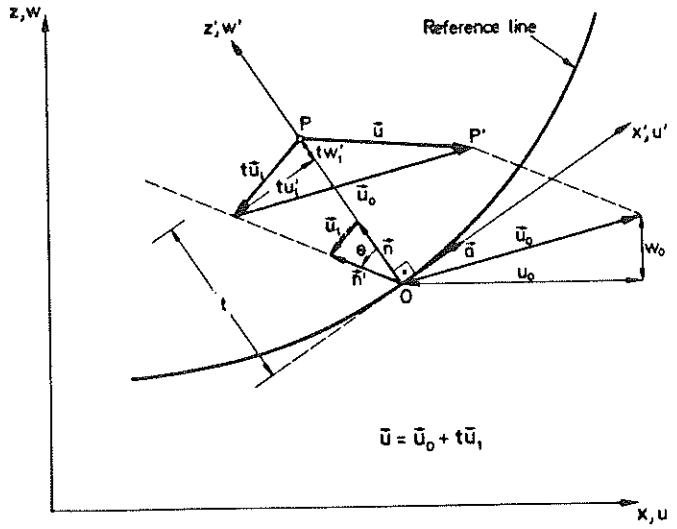

Fig. 7 Definition of displacement field

6.3. Strain-displacement relationships.

Vector **g** is defined as

$$\mathbf{g} = \begin{Bmatrix} g_1 \\ g_2 \end{Bmatrix} \tag{66}$$

where $g_1 = [\, g_1 \;,\; g_3 \,]^T$ and $g_2 = [\, g_7 \;,\; g_9 \,]^T$

where g_1 , g_3 , g_7 and g_9 are the same as in eq (14). The Green strain vector is obtained as

Arches **Axisymmetric shells**

$$\epsilon^A = \begin{Bmatrix} \epsilon_{x'} \\ \gamma_{x'z'} \end{Bmatrix} = \begin{Bmatrix} g_1 + \tfrac{1}{2}(g_1^2 + g_3^2) \\ g_3 + g_7 + g_1 g_7 + g_3 g_9 \end{Bmatrix}; \quad \epsilon^{AS} = \begin{Bmatrix} \epsilon^A \\ \epsilon_{y'} \end{Bmatrix} = \begin{Bmatrix} \epsilon^A \\ g_5 + \tfrac{1}{2} g_5^2 \end{Bmatrix} \tag{67}$$

with $g_5 = \dfrac{u}{\rho}$ and ρ is defined in Fig. 6.

It can be shown that [13]

$$g = L\, P \tag{68}$$

with

$$L^A = \left[\begin{array}{c|c} C_r\, T\, \dfrac{d}{d_r} & t C_r \left(\Delta + I_2 \dfrac{d}{d_r} \right) \\ \hline 0 & I_2 \end{array}\right]; \quad L^{AS} = \begin{bmatrix} L^A \\ \dfrac{1}{\rho}; o, \dfrac{t}{\rho}\cos\phi, -\dfrac{t}{\rho}\sin\phi \end{bmatrix} \tag{69}$$

with

$$\Delta = \frac{1}{R} \begin{bmatrix} 0 & -1 \\ 1 & 0 \end{bmatrix} \quad , \quad C_r = \frac{1}{1 - \dfrac{t}{R}} \tag{70}$$

The obtention of the different incremental relationships between strains and displacements follows identical steps as explained for 3-D shells. Options 1, 2 and 3 for defining the finite element interpolation forms in sections 3.1 , 3.2 and 3.3 respectively are again possible. The obtention of the different matrices follows the pattern described in those sections and it will not be repeated here. More details of the resulting expressions for C_i , G_i, ^{A} and B_i matrices can be found in [13].

6.4. Tangent matrix.

The different expressions for the tangent matrix are identical to those presented in eqs (53) - (56) for 3-D shells. However, matrix S of eq (55) is now given by

Arches **Axisymmetric shells**

$$S^A = \begin{bmatrix} \sigma_{x'}\, I_2 & \tau_{x'z'}\, I_2 \\ \text{Sym.} & 0 \end{bmatrix} \qquad S^{AS} = \begin{bmatrix} S^A & o \\ 0 & \sigma_{y'} \end{bmatrix} \tag{71}$$

and matrix H_i of eq (56) is obtained for both cases (using the interpolation option 1 of section 3.1) as

$$H_i \ (1 \times 1) = \int_V \frac{\partial g_i^T}{\partial \theta_i} \ A^T \sigma dV \qquad (72)$$

where g_i is the last colum of matrix G_i (see ref.[13]).

It is worth noting that the volume integrals of the 3D formulation are now transformated into the following area integrals.

Arches	Axisymmetric shells
$\int_A f(x\ ,\ z)\, b dA$	$2\pi \int_A f(x\ ,\ z)\, \rho\, dA$

where b is the width of the arch (see Fig. 6).

Finally, the corresponding geometricaly non linear formulation for framed structures can be directly obtained from the arch formulation simply making the curvature radius R equal to infinity in the all appropiate terms of the finite element matrices. However, direct use can be made of the arch formulation for analysis of frames setting a cut off value for R in the numerical computations.

6. NUMERICAL EXAMPLES

A series of examples which show the efficiency of the formulation developed are presented next. The elements used here for the different structures analyzed are the eight noded isoparametric element which a 2 x 2 x 2 reduced integration rule for the 3D shell example and the three noded isoparametric one dimensional element, also with a reduced 2-2 integration rule for the axisymmetric shell, arch and frame examples. However, any of the well know members of the "thick shell element" family recently developed [23],[24]could also be used.

6.1. 3D shells: Cylindrical shell under point load.

The cylindrical shell studied can be seen in Fig. 8. Note that only four elements have been used to discretise one quarter of the structure (due to symmetry). The shell is assumed to be simply supported in its straight edges and free in the curved ones. Fig. 8 also shows the load-displacement paths obtained for two points A and B of the structure for a shell thickness of 12,7 mm. Good comparison with results reported by Sabir and Lock [8] and Surana [7], also shown in Fig. 8 is obtained. Note the unexpected good performance of the eight noded element for

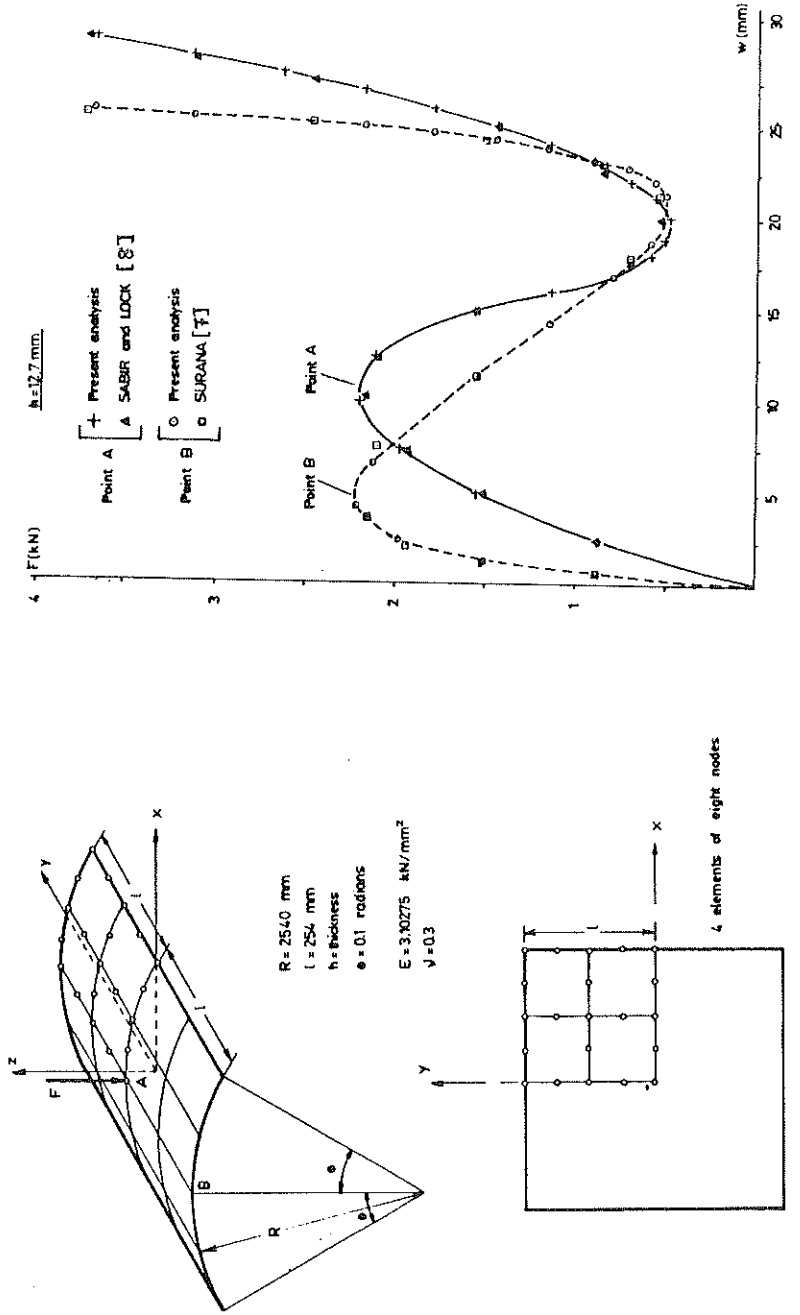

Fig.8 Cylindrical shell under point load.

a relatively "thin" shell structure (t/R = 0,005). Similar good results for this element obtained with the formulation presented here have been recently reported by the authors [12].

6.2. Axisymmetric shells: Expansion below under end circular point load.

A segment of an expansion below under circular point load acting at both ends has been analyzed with the axisymmetric formulation presented in section 5. The geometry of the cross section of the segment analyzed, material properties and the two meshes of 3 and 6 three noded axisymmetric elements used in the analysis are shown in Fig. 9. Results obtained for the load-deflection curve relating the vertical displacement δ at the end A with the total circular load applied F are presented in Fig.9. It can be seen that numerical results obtained with the 3 element mesh are very accurate in comparison with those obtained by Nayak [19] and Surana [20], also shown in Fig. 9, using a considerably higher number of elements.

6.3. Arches: Simply supported circular arch under point load.

The formulation for arches presented in section 5 has been applied to the analysis of a circular arch under a vertical point load acting at the center. The arch geometry, material properties and finite element mesh of 10 three noded elements used are shown in Fig. 10. Numerical results obtained for the load-central deflection curve are also shown in Fig. 10. This problem presents a bifurcation point A shown in Fig. 10. The corresponding symmetrical and non symmetrical deformation modes have been plotted in Fig. 10 . Numerical results obtained for the two bifurcation branches of the load-deflection curve (see Fig. 10) compare well with those reported by Huddleston [17]for the same problem.

6.4. Framed structures: Rectangular frame under end point loads.

The arch formulation developed in section 5 can also be applied to the case of framed structures as shown in this last example. The geometry of the structure and details of the material properties can be seen in Fig. 11 . Only one quarter of the structure has been analysed due to the symmetry of the problem. 10 onedimensional three noded elements have been used in the analysis (see Fig. 11). Numerical results for the load-deflection and central bending moment-deflection curves are shown in Fig. 11 where results obtained by Lee [18]for this problem have also been plotted. Comparison between both set of results is good. It is worth noting that an elastoplastic analysis has also been carried out for this problem using the same one dimensional formulation derived in section 5. For the plastic properties a simple von Mises non hardenning material has been assumed. The value of the yield stress has been taken equal to 10^5 N/m^2. Results for the elastoplastic load and bending moment versus deflection paths are also presented in Fig. 11 . Finally, the spread of the

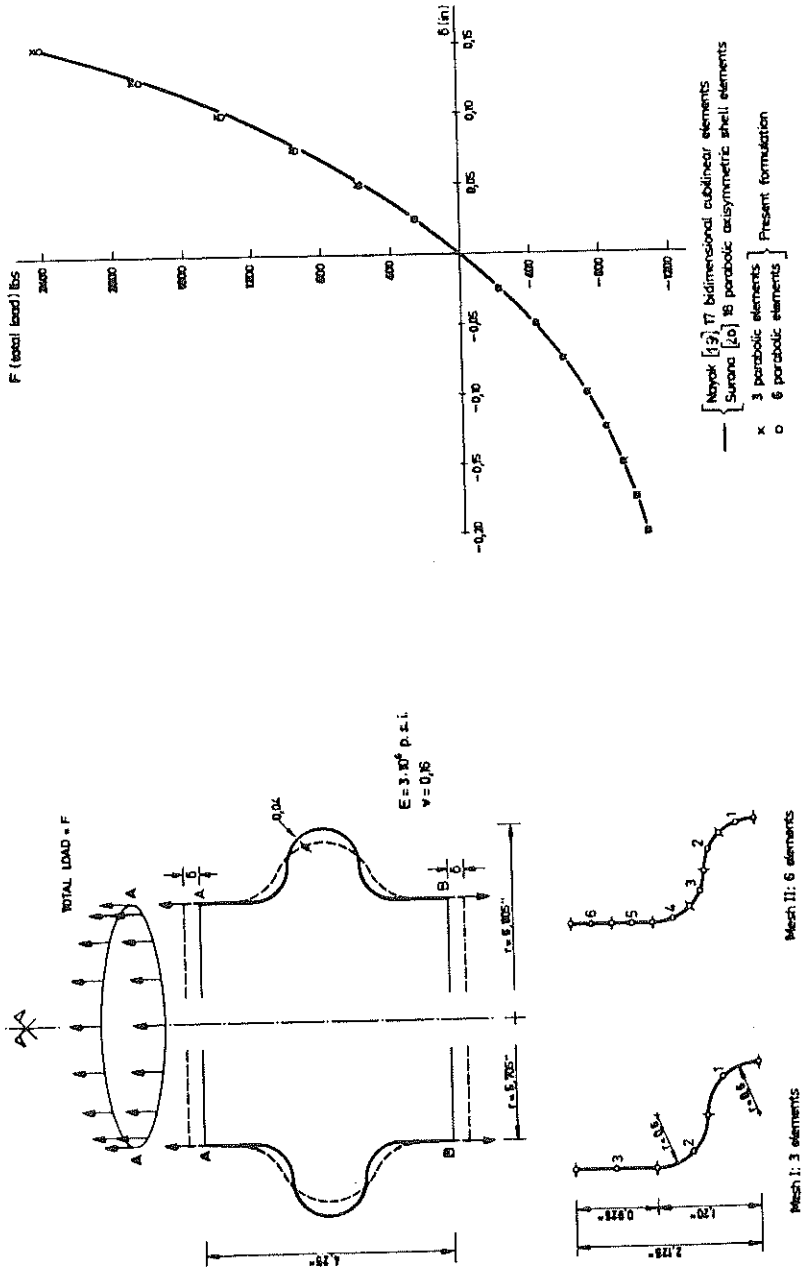

Fig.9 Expansion below under end circular point load.

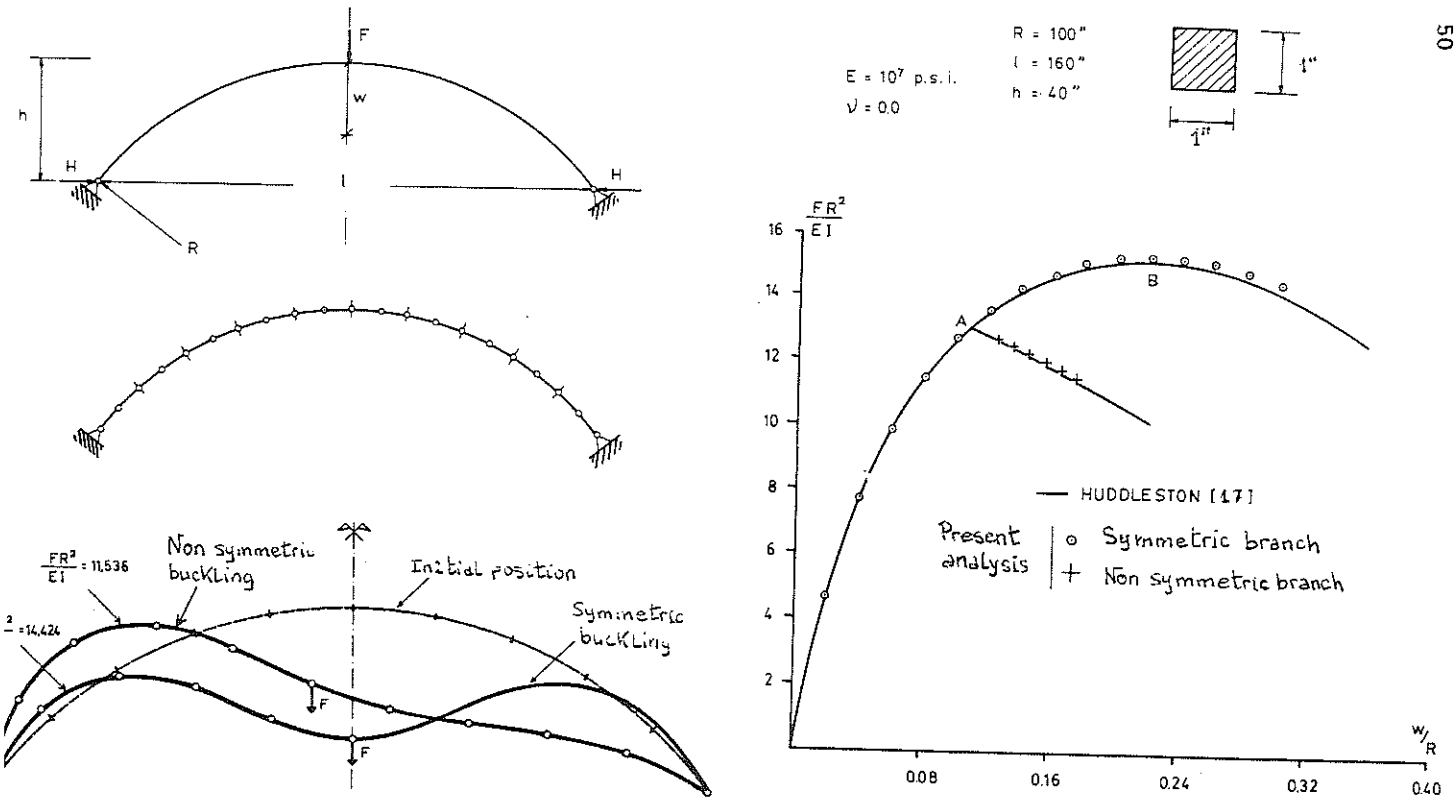

Fig.10 Simply supported circular arch under point load.

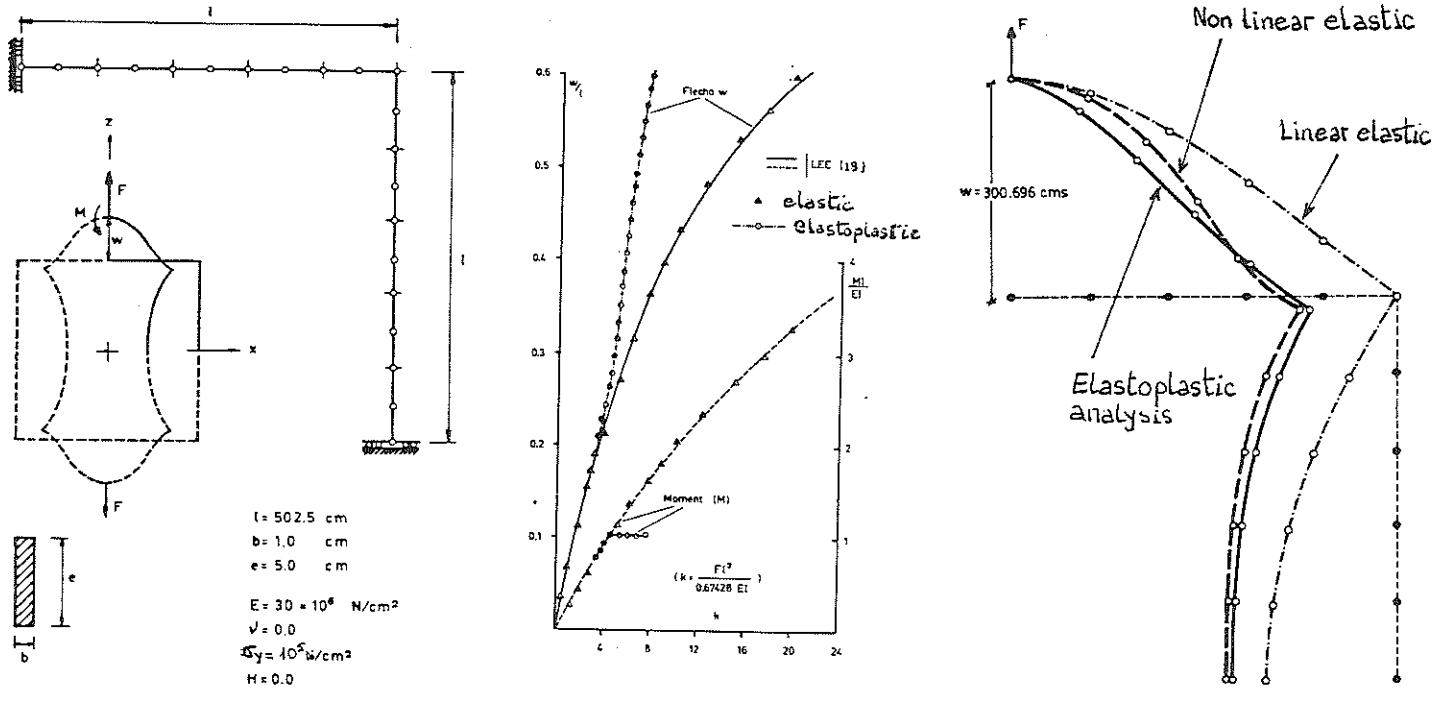

Fig.11 Rectangular frame under point load

plastic zones for a vertical deflection of 258.05 cm. is shown in Fig. 12 More details about this problem can be found in reference [11].

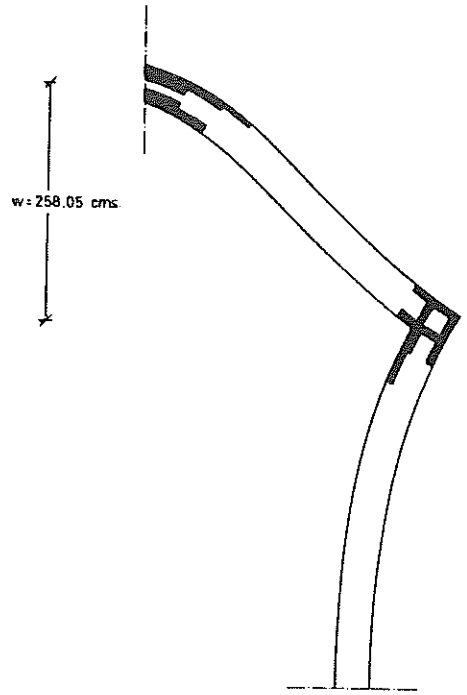

Fig. 12 Rectangular frame: Development of plastic zones

8. FINAL REMARKS

A Total Lagrangian finite element formulation for the geometricaly non linear analysis of shell, arch and frame structures has been presented. The formulation allows for large displacement and rotations along the deformation path of the structure. Different alternatives for defining the finite element interpolation parameters and the corresponding deformation matrices obtained have been studied. It has also been shown how the general non linear 3D shell formulation is a good starting point for deriving simplified forms for the 2D analysis of axisymmetric shells, arches and frames. The examples presented show the efficiency of the formulation for the analysis of a variety of different practical structural problems. Extensions of this work could easily include the obtention of a non linear formulation for spatial rods which could also be obtained as a particular case of the 3D shell formulation presented in this chapter. An application of the arch formulation to the non linear analysis of marine pipelines during laying operations has been recently published by the authors [21] .

REFERENCES

1. Argyris, J.H., Balmer, H., Kleiber, M. and Hindenlang, U. Natural description of large inelastic deformation for shells of arbitrary shape-Applications of trump element. Computer Meth. Appl. Mech. Engng. 22,361-389, 1980.

2. Chang, T.Y. and Sawamiphakdi, Large deflection and post-buckling analysis of shell structures, Comp. Meth. Appl. Mech. Engn. 32, 311-326, 1982.

3. Bathe, K.J. and Bolourchi, S., A geometric and material non linear plate and shell element. Computer and Structures, **11**, 23-48, 1980.

4. Bathe, K.J. and Ho, L.H., A simple and effective element for analysis of general shell structures, Computer and structures, **13**, 673-681, 1981.

5. Hughes,T.J.R.and Liu, W.K., Non linear finite element analysis of shells. Part I: Three dimensional shells. Comp.Meth. Appl. Mech. Engng. 26, 331-362, 1981.

6. Hughes,T.J.R.and Liu, W.K. Non linear finite element analysis of shells. Part II: Two dimensional shells. Comp. Meth. Appl. Mech. Engng., 27, 167-181, 1981.

7. Surana, K.S., Geometricaly non linear formulation for the curved shell element. Int. J. Num. Meth. Engng, **19**, 581-615, 1983.

8. Sabir, A.B. and Lock, A.C. The application of finite elements to the large deflection geometrically non linear behaviour of cylindrical shells. Variational Methods in Engineering. Ed. Brebbia and Tottenham, Southampton. Univ. Press, 7, 66-75. 1973.

9. Ramm, E. A plate shell element for large deflection and rotations. Formulation and Computational Algorithms in Finite Element Analysis. Eds. K.J. Bathe, J.T. Oden and W. Wundeslich, M.I.T. Press, 1977.

10. Wood, R.D. and Zienkiewicz, O.C. Geometrically non linear finite element analysis of beams, frames, arches and axisymmetric shells. Comp. Struct. 7, 725-735, 1977.

11. Oliver, J. Una formulación cuasi-intrínseca para el estudio por el método de los elementos finitos de vigas, arcos, placas y láminas sometidas a grandes corrimientos en régimen elastoplástico. Ph. Thesis. Univ. Politech. Cataluña, Spain 1982.

12. Oliver, J. and Oñate, E. A Total Langrangian formulation for the geometrically non linear analysis of structures using finite elements. Part I: Two dimensional problems: shell and plate structures. Int. J. Num. Meth. Engng. **20**, 2253-2281, 1984.

13. Oliver, J. and Oñate, E. A Total Lagrangian formulation for the geometrically non linear analysis of structures using finite elements. Part II: Arches, frames and axisymmetric shells. Int. J. Num. Meth. Engng. (In press).

14. Oñate, E. and Oliver, J. A Total Lagrangian finite element formulation for the large displacement/large rotation analysis of 3-D shells, arches and axisymmetric shells. Proc. of the II Int. Conf. in Num. Meth. Non Linear Prob. Eds.C. Taylor et al. Pineridge Press, **2**, 152-169, 1984.

15. Crisfield, M.A. Incremental/iterative solution procedures for non linear structural analysis. Proc. Int. Conf. Num. Meth. Non Linear Prob. Eds. C. Taylor et al, Pineridge Press (1).

16. Zienkiewicz, O.C. The finite element method. McGraw Hill, 1977.

17. Huddeston, J.V. Finite deflection and snap though of nigh circular arches. Journal Appl. Mech. June, 1969.

18. Lee, S.L., Manuel, F.S. and Rossow, F.G. Large deflection and stability of elastic frames. Journal ASCE. Engng. Mech. Div., **94**. 2, April, 1968.

19. Nayak, C.Ch. Plasticity and large deformation problems by the finite element method. Ph. D. Thesis. University of Wales, Swansea, 1971.

20. Surana, K.S. Geometrically non linear formulation for axisymmetric shell elements. Int. J. Num. Meth. Engng. **18**, 477-502, 1982.

21. Oliver, J. and Oñate, E. A finite element formulation for the analysis of marine pipelines during laying operations. Journal of Pipelines, **5**, 15-35, 1985.

22. Numerical methods of forming processes. J.Pittman et al eds., J.Wiley (1984).

23. Tessler,A. and Hughes, T.J.R. An improved treatment of transverse shear in the Mindlin type four node quadrilateral element. Comp. Meth. Appl. Mech. Engng, **39**, 311-335, 1983.

24. Dvorkin, E.N. and Bathe, K.J. A continuum mechanics based four node element for general non linear analysis. Engn.Comput. **1**, 77-88, 1984.